

## Structural and Functional Characterization of Human Immunodeficiency Virus *tat* Protein

STEVEN RUBEN,<sup>1</sup> ANN PERKINS,<sup>1</sup> RICHARD PURCELL,<sup>2</sup> KEITH JOUNG,<sup>3</sup> REY SIA,<sup>3</sup> ROBERT BURGHOFF,<sup>3</sup> WILLIAM A. HASELTINE,<sup>3</sup> AND CRAIG A. ROSEN<sup>1\*</sup>

Department of Molecular Oncology, Roche Institute of Molecular Biology,<sup>1</sup> and Department of Protein Chemistry, Hoffmann-La Roche Inc., Roche Research Center,<sup>2</sup> Nutley, New Jersey 07110, and Department of Pathology, Dana-Farber Cancer Institute, Harvard Medical School, Boston, Massachusetts 02115<sup>3</sup>

Received 21 July 1988/Accepted 19 September 1988

Site-directed mutagenesis was used to identify functional domains present within the human immunodeficiency virus (HIV) *tat* protein. Transient cotransfection experiments showed that derivatives of *tat* protein with amino acid substitutions either at the amino-terminal end or at cysteine residue 22, 37, 27, or 25 were no longer able to transactivate HIV long terminal repeat-directed gene expression. Incubation of Tat expressed in *Escherichia coli* with zinc demonstrated that both authentic Tat and cysteine mutation derivatives could form metal-protein complexes. The *tat* proteins that contained alterations within the cluster of positively charged amino acid residues retained their ability to transactivate gene expression, albeit at markedly reduced levels. Indirect immunofluorescence showed that the authentic *tat* protein and the amino-terminal and cysteine substitution mutants all localized in the nucleus, with accumulation being most evident in the nucleolus. In contrast, nuclear accumulation was greatly reduced with the basic-substitution mutations. Consistent with this result, a fusion protein that contained amino acids GRKKR, derived from the basic region, fused to the amino-terminal end of  $\beta$ -galactosidase also accumulated within the nucleus. These results demonstrate that the 14-kilodalton *tat* protein contains at least three distinct functional domains affecting localization and transactivation.

Human immunodeficiency virus (HIV) encodes several *trans*-acting regulatory proteins not present in other retroviruses. One of these genes, designated *tat*, encodes a 14-kilodalton (kDa) nuclear protein that acts in *trans* to stimulate virus gene expression (1, 25). Expression of *tat* is required for replication (6, 8). The *cis*-acting sequences responsive to *tat*, referred to as TAR (for *trans*-acting responsive region), are present between nucleotides -17 and +80 in the long terminal repeat (LTR) (20). As such, the TAR sequences are present in both the DNA and 5' untranslated leader region of all HIV mRNAs. Expression of heterologous genes that contain the TAR sequences at their 5' end is also greatly elevated in the presence of Tat. The 5' end of the HIV mRNAs can form a stable stem-loop structure, which has been proposed to be a binding site for Tat (15). However, no specific binding of Tat to this region has been identified. The mechanisms by which Tat regulates HIV gene expression have proven to be complex. Several mechanisms have been proposed to explain the *trans*-acting activity, including increased mRNA stability, differential transport, enhanced utilization of transcribed mRNA, and abatement of transcription termination within the TAR region (4, 7, 11, 15, 18, 19, 20, 27). Thus, both transcriptional and posttranscriptional mechanisms have been proposed for Tat function.

To gain insight into Tat function, we used site-directed mutagenesis to identify regions important for function. Our results demonstrate that the *tat* protein contains at least three functional domains, two of which are required for transactivation and a third which contains a nuclear localization signal similar in structure to previously identified nuclear localization sequences.

### MATERIALS AND METHODS

**Construction of expression vectors.** For expression of Tat in eucaryotic cells, the vector pictured in Fig. 2A was used. Plasmid pSVEX contains the simian virus 40 (SV40) early-region promoter, followed by a multiple-restriction-site polylinker (obtained from plasmid SP6, Promega Biotec) and SV40 polyadenylation signals obtained from plasmid pSVGT5-Ra $\beta$ G (16). For expression of authentic Tat, the *Sall*-*Bam*HI fragment extending from nucleotides 5332 to 8020 of strain HXBC2 was inserted into the *Sall*-*Bg*III site present on plasmid pSVEX. For expression of mutant *tat* proteins, the same cloning strategy was followed.

For procaryotic expression, the *Xho*II-*Hind*III *tat* fragment of strain HXBC2 was cloned into the procaryotic expression vector pDS56/RBS11-1 (2) shown in Fig. 2B.

For expression of  $\beta$ -galactosidase fusion proteins, synthetic oligonucleotides encoding the amino acids pictured in Fig. 2C were synthesized with 5' *Hind*III and 3' *Bam*HI overhangs. Oligonucleotides were ligated to a *Bam*HI-*Sall* DNA fragment containing the *lacZ* gene of *Escherichia coli*, and the resultant DNA fragment was cloned into the *Hind*III-*Sall* site of plasmid pSVEX.

**Site-directed mutagenesis.** To obtain single-stranded DNA corresponding to the coding sequence of *tat*, a *Sall*-*Bam*HI fragment encompassing nucleotides 5332 to 8020 of strain HXBC2 was cloned into the replicative form (RF) of phage M13mp9 (New England Biolabs). Infected cells were grown to saturation, and single-stranded DNA was isolated from phage. Oligonucleotides used in mutagenesis were synthesized on an Applied Biosystems DNA synthesizer. Oligonucleotides were deprotected with ammonium hydroxide at 55°C overnight, isolated on 20% polyacrylamide gels containing 7 M urea, eluted overnight in 1 M triethylamine buffer, pH 7.4, and desalted over SEP-PAK C14 columns (Waters Associates). Labeled probes for hybridization

\* Corresponding author.

screening were made by treating oligonucleotides with kinase in the presence of  $\gamma$ - $^{32}\text{P}$ -labeled ATP to a specific activity of 100 to 300 cpm/pg. For mutagenesis, the procedure followed was adapted from that of Nesbit and Beilharz (17). Briefly, oligonucleotide-directed mutagenesis was performed by annealing the desired kinase-treated primer and universal M13 sequencing primer (New England Biolabs) to the appropriate single-stranded M13 DNA template, extending the primer strand with DNA polymerase I large fragment, and ligating the synthesized strand with T4 DNA ligase to generate covalently closed, circular, double-stranded RFs with the 1-base-pair (bp) mismatch. To reduce the background resulting from residual unconverted single-stranded DNA, the mixture of covalently closed circular DNA and single-stranded DNA was phenol-chloroform extracted, ethanol precipitated, and incubated with *Pst*I and *Sac*I for 3 h to generate the fragment containing the *tat* gene with the 1-bp mismatch. This mixture was then added to the *Pst*-*Sac*I-digested plasmid pTZ 18U (U.S. Biochemicals) and incubated overnight with T4 DNA ligase. The ligation reaction mix was transformed into competent *E. coli* JM101, and one-third of the transformation mixture was plated on 5-bromo-4-chloro-3-indolyl- $\beta$ -D-galactoside indicator plates (to check for the presence of inserts in the pTZ18U plasmid), and the remaining two-thirds were grown overnight in 10 ml of LB broth. If a large percentage of white colonies were evident, DNA was extracted from the overnight culture and used for a second transformation. The resultant colonies were screened for the presence of the desired mutation. To screen for the presence of a single-base-pair mismatch, the oligonucleotide used in creating the mutant was treated with kinase and [ $\gamma$ - $^{32}\text{P}$ ]ATP and used to screen a set of possible mutants. Ninety-six-well plates containing 200  $\mu\text{l}$  of LB freezing medium were inoculated with the individual colonies, which were grown overnight and replica plated onto LB agar plates containing ampicillin (100  $\mu\text{g}/\text{ml}$ ). Plates were incubated at 37°C overnight, and colonies were lifted with Whatman 541 paper.

The hybridization procedure used was adapted from that of Wood et al. (26), with tetramethyl ammonium chloride used in the washings. The use of tetramethyl ammonium chloride eliminates differences in the bond energies of A:T and G:C pairs and allows calculation of the temperature of dissociation ( $T_d$ ) directly from the length of DNA without considering base composition. Four different filters for each set of clones were washed at four different temperatures, above and below the predicted  $T_d$ . Clones that remained hybridized under stringent temperatures were selected for dideoxy chain termination sequencing (22). Fragments from clones containing the desired insert were then cloned into the expression vector pSVEX.

**Cell transfection and CAT assays.** The functional activity of each *tat* mutant was assessed by chloramphenicol acetyltransferase (CAT) assays following transfection of HeLa cells. In general, cells were seeded 24 h prior to transfection at a density of  $10^6$  per 100-mm dish. Transfection was achieved with a modified DEAE-dextran-calcium phosphate protocol. Briefly, the desired amount of DNA was mixed with 475  $\mu\text{l}$  of transfection solution (137 mM NaCl, 5 mM KCl, 0.3 mM  $\text{Na}_2\text{HPO}_4 \cdot 7\text{H}_2\text{O}$ , 2.4 mM Tris chloride [pH 7.4] plus 1/100 volume of  $\text{MgCl}_2$ - $\text{CaCl}_2$  solution [10 mg of  $\text{MgCl}_2$  and  $\text{CaCl}_2$  per ml]) plus 10  $\mu\text{l}$  of DEAE solution (10 mg of DEAE-dextran per ml in water) and incubated for 15 min at room temperature. Medium was removed from plates, and cells were washed once and then overlaid with fresh medium and serum. At 48 h following transfection, the

medium was removed, and the cells were washed with phosphate-buffered saline (PBS) and suspended in 150  $\mu\text{l}$  of 250 mM Tris (pH 8.0). Cells were subjected to three freeze-thaw cycles ( $-70$  and  $37^\circ\text{C}$ , respectively) and centrifuged to remove cell debris. Then, 35  $\mu\text{l}$  of the cell extract was incubated with 5  $\mu\text{l}$  of chloramphenicol reaction mix (24 mM acetyl coenzyme A, 0.1  $\mu\text{Ci}$  of [ $^{14}\text{C}$ ]chloramphenicol) at  $37^\circ\text{C}$ . The reaction was quenched with the addition of ethyl acetate, and the organic layer was removed, lyophilized, suspended in 20  $\mu\text{l}$  of ethyl acetate, and spotted onto thin-layer chromatography plates (9). Autoradiograms were produced by overnight exposure of the dried plate.

**Indirect immunofluorescence.** COS-7 cells were plated at a density of  $10^5$  cells per 35-mm dish 24 h prior to transfection. Cells were transfected with 1  $\mu\text{g}$  of plasmid DNA by the DEAE-dextran transfection procedure as described previously (5), except that the chloroquine step was omitted. At 48 h posttransfection, cells were washed with PBS, fixed in 3% paraformaldehyde in PBS (pH 7.8) for 30 min at room temperature, washed for 5 min in PBS plus 10 mM glycine, incubated for 5 min with 1% Triton X-100 in PBS, washed again for 5 min, incubated with 25 mM glycine for 30 min, washed, and finally blocked with 3% goat serum (Vector Laboratories) in Western antibody buffer (1% bovine serum albumin in PBS, pH 6.5, with 0.5 M NaCl and 0.05% Tween-20) for at least 1 to 5 h at room temperature. Additional nontransfected cells were treated with the same procedure up to this point, and the *tat* antibody prepared against a peptide corresponding to amino acids 67 to 87 was preabsorbed to the cells during incubation. After blocking, the preabsorbed *tat* antibody was diluted in Western antibody buffer to a concentration of 1:300 and added to the cells. Cells were incubated at  $4^\circ\text{C}$  overnight. The following day, cells were washed twice with PBS containing glycine for 10 min each and then incubated in the dark with rhodamine isothiocyanate-conjugated goat anti-rabbit immunoglobulin G secondary antibody diluted 1:100 in Western antibody buffer plus 1% goat serum with gentle shaking at room temperature for 1 h. Cells were washed three times with PBS containing glycine. Cover slips were mounted, and cells were viewed with a light fluorescent microscope. A similar procedure was used for localization of the  $\beta$ -galactosidase fusion proteins, except that preabsorption of antibody was not done.

**Zinc blotting and autoradiography.** The procaryotic *tat* expression vectors were grown to an  $\text{OD}_{600}$  of 0.6, and *tat* expression was induced by addition of 1 mM isopropylthiogalactopyranoside (IPTG). After an additional 4 h of growth, cells were centrifuged and lysed, and proteins were separated by sodium dodecyl sulfate-polyacrylamide gel electrophoresis (SDS-PAGE). Proteins were electrophoretically transferred to nitrocellulose with a Bio-Rad Transblot apparatus. After transfer to nitrocellulose, the filters were washed in metal-binding buffer and probed for 1 h with  $^{65}\text{ZnCl}_2$  as described by Shiff et al. (23).

## RESULTS

To identify functional domains within the *tat* protein, site-directed mutagenesis was used to introduce single-amino-acid substitutions. Substitutions were introduced within a truncated form of *tat* protein encoded by the first exon. Previous studies have shown that the first 58 amino acids are sufficient for full activity (24). Mutations introduced within the *tat* gene are shown in Fig. 1. Initially, three regions were chosen for mutagenesis: the amino-terminal

**A**

MEPVDPRLPEWKHPGSQ  
1

PKTACTNCYCKKCCFHC  
22 25 27

QVCFITKALGISYGRKK  
37 5051

RRQRRRPPQGSQTHQ STOP  
55

**B**

Plasmid	Mutations		Activity
	Amino Acid Original	→ New	
pC22	C	S	-
pC25	C	R	-
pC27	C	S	-
pC37	C	S	-
pK50-S	K	Stop	-
pKK5051	KR	SG	+
pR55	R	G	+
pEPV	EPV	R	-

FIG. 1. (A) Amino acid sequence of the first exon of the *tat* protein and (B) mutations created. The numbers below the amino acids refer to the amino acid position relative to the methionine present at position 1. (B) Plasmids are named according to the amino acid that was mutated. The activity denotes the ability of the mutant protein to activate HIV LTR-directed gene expression (see Fig. 4)

domain, the cysteine-rich domain, and amino acids present within the positively charged domain. For mutagenesis, a genomic fragment spanning nucleotides 5332 to 8020 from plasmid HXBC2 was subcloned into the RF of phage M13. Single-stranded DNA was prepared and mutagenesis was performed as described in the Materials and Methods section. Following identification of clones containing the desired mutation, the DNA encoding the *tat* region was subcloned into the eucaryotic and procaryotic expression vectors shown in Fig. 2. The functional activity and subcellular localization of each Tat derivative were assessed as described below.

**Subcellular localization of the *tat* protein.** Prior to analysis of the mutant *tat* proteins, the subcellular localization of Tat was determined. Previously, Hauber et al. demonstrated that Tat is localized in the nucleus (11). To determine the subcellular localization of Tat, COS cells were transfected with plasmid pSV*tat* and subjected to indirect immunofluorescence analysis 48 h posttransfection. In this vector system (Fig. 2A), a high level of transient gene expression is achieved through replication of plasmid DNA containing the SV40 origin of replication by SV40 T antigen which is constitutively expressed in the COS cell line. As shown in Fig. 3A and B, the *tat* protein was localized in the nucleus,

in accord with previous findings. Moreover, the majority of *tat* protein was sequestered within the nucleolus under these conditions. Nucleolar staining was also apparent in the absence of accumulation in the nucleoplasm. Experiments done in parallel with a *c-fos* expression vector or a nucleus-targeted  $\beta$ -galactosidase fusion protein (see below) gave the expected nuclear localization and nucleolar exclusion, indicating that the nucleolar localization observed with the *tat* protein was not an artifact of the procedure.

**Several functional domains are present in the *tat* protein.** The activity of the individual mutant *tat* derivatives was assessed by using transient cotransfection assays with plasmid pU3R-III, which contains the bacterial *cat* gene under the control of the HIV LTR (20). Transfections were performed in HeLa cells, and CAT activity was measured at 48 h posttransfection. As expected, cotransfection of pU3R-III with plasmid pSV*tat*, which carries the first exon of *tat*, led to stimulation of LTR-directed *cat* gene expression (Fig. 4). Transactivation was completely abolished with the amino-terminal (plasmid pEPV) and cysteine substitution mutations (C22, C25, C27, and C37). Similar results were obtained following cotransfection of human T4 lymphoid Jurkat cells and CHO cells (not shown). Loss of transactivation with these mutant proteins suggests a structural defect in a functional domain, since expression and proper subcellular localization of the mutant proteins were maintained (see below).

In contrast with the above findings, cotransfection with plasmids containing substitutions or deletions of the basic residues (50, 55, and 50-51) gave two phenotypes. At saturating amounts of expression vector DNA, activity was 10 to 20% of that observed with wild-type DNA (Fig. 4). However, at nonsaturating amounts of DNA, the activity of the proteins expressed from plasmids pR55 and pKK5051 was markedly reduced. For example, in the range from 1 to 0.1  $\mu$ g, plasmid pKK5051, which contains the Lys-Lys to Ser-Gly substitution, retained only 1/100 the activity of an equivalent amount of plasmid pSV*tat* (data not shown).

**Subcellular localization of mutant *tat* proteins.** To identify the subcellular localization of the individual mutant proteins, plasmids were transfected into COS cells and the subcellular localization of Tat was examined by indirect immunofluorescence at 48 h posttransfection. Both the amino-terminal substitution mutant, expressed from plasmid pEPV, and the cysteine substitution mutants were localized within the

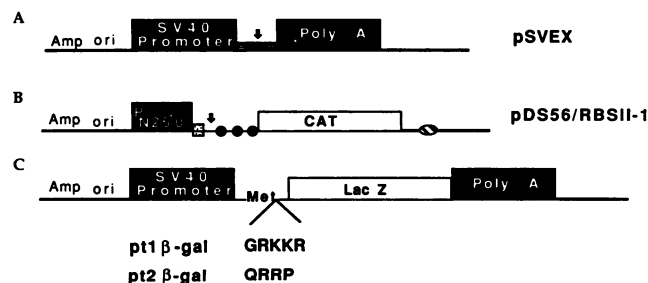


FIG. 2. Eucaryotic and procaryotic expression vectors. The pSVEX eucaryotic expression vector is described in the text. The pDS56RBS11-1 procaryotic expression vector contains a ribosome-binding site (hatched box) following the promoter, and a stop codon (solid circle) in each reading frame follows the cloning site (2). A termination signal follows the *cat* gene. Expression of the  $\beta$ -galactosidase fusion proteins was achieved by cloning the hybrid  $\beta$ -galactosidase gene DNA fragments (see text) into the cloning site present in plasmid pSVEX.

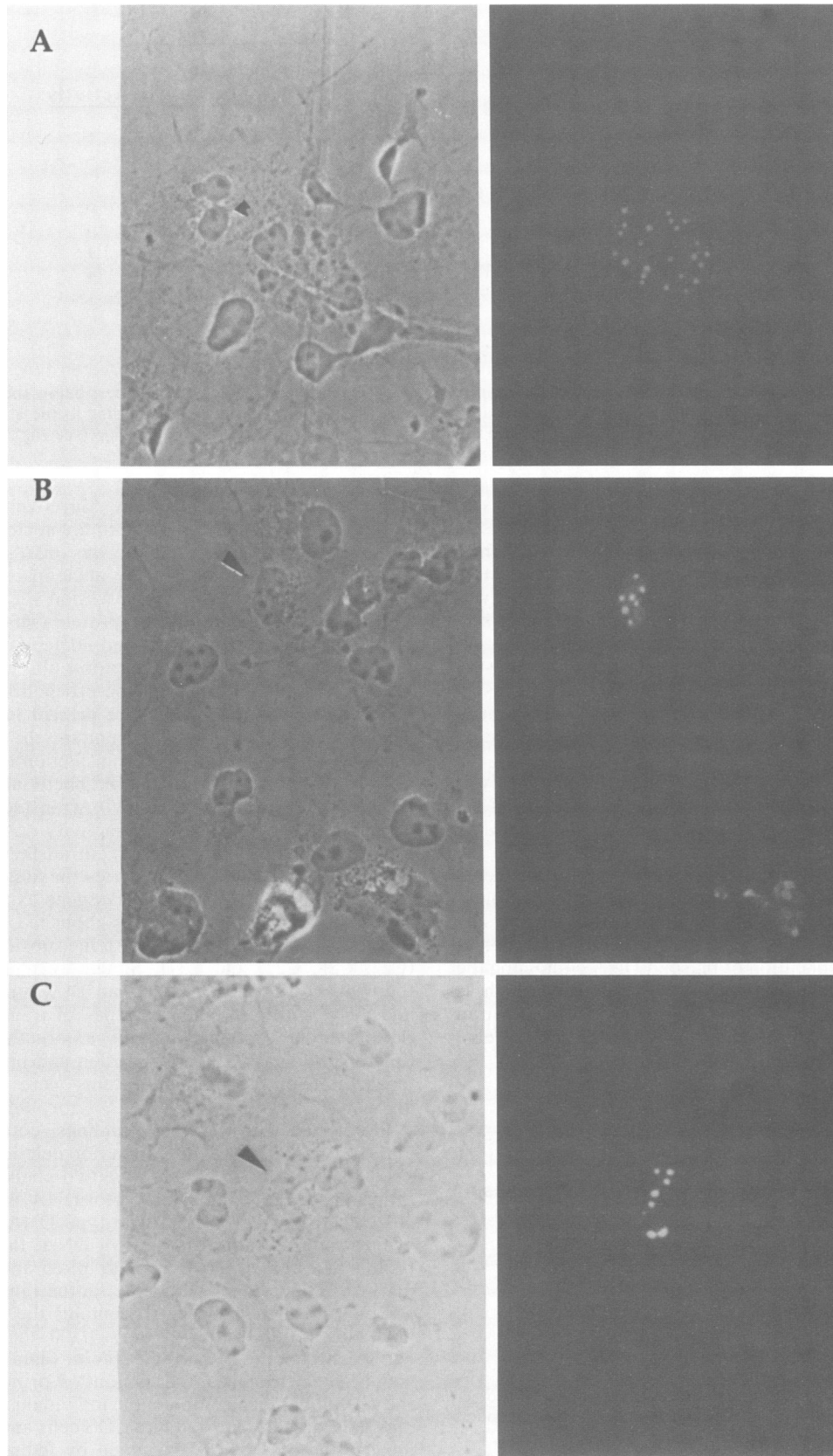


FIG. 3. Indirect immunofluorescence staining of COS-7 cells expressing authentic *tat* protein. COS cells were transfected with 1  $\mu$ g of plasmids pSV*tat* (A), pC22 (B), and pC27 (C) and stained 48 h posttransfection as described in the text. Phase-contrast (left) and fluorescence (right) photomicrographs are shown. Arrows mark the perimeter of the cell.

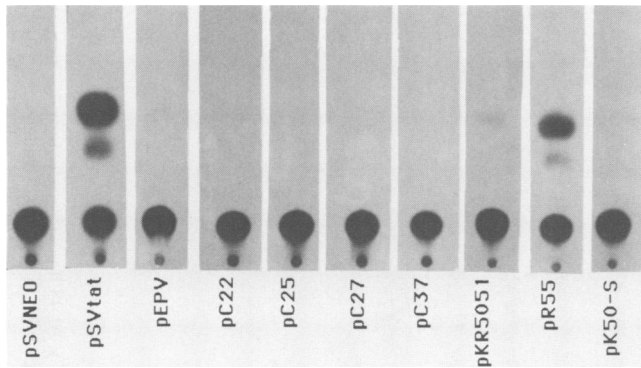


FIG. 4. Activity of the mutant *tat* proteins in HeLa cells. The series of *tat* expression vectors shown in Fig. 1 were cotransfected with plasmid pU3R-III into HeLa cells. CAT assays were performed 48 h posttransfection. An autoradiogram obtained from a 30-min reaction is shown.

nucleus, with accumulation most evident in the nucleolus. Representative photomicrographs are shown in Fig. 3. The proteins that contained substitutions at the basic residues, although expressed, as indicated by their ability to transactivate, could not be localized accurately by indirect immunofluorescence, perhaps because the level of accumulation in the nucleus was below the level of detection with our antisera.

**Identification of nuclear localization signals.** Localization of Tat within the nucleus raised the possibility that this protein contained a distinct nuclear localization sequence. The diminished ability of the mutant proteins with substitution of the basic residues to transactivate gene expression and the lack of detectable protein in the nucleus suggested the presence of a potential nuclear localization signal within this region.

Regions important for nuclear localization have been identified for several viral and cellular proteins (3, 12). Although no definitive structure has been identified, a number of continuous positively charged residues are often present within the localization sequence (3, 12). Therefore, the ability of the basic residues of Tat to function as a nuclear localization or accumulation signal was examined. For these studies, we tested the ability of the basic residues to direct the heterologous 116,000-kDa  $\beta$ -galactosidase protein, encoded by the *lacZ* gene of *E. coli*, to the nucleus. A similar approach has been used to identify other nuclear targeting signals (12).  $\beta$ -Galactosidase fusion proteins with the general structure shown in Fig. 2C were constructed in the SV40-derived expression vector. Subcellular localization was determined 48 h posttransfection of COS cells by indirect immunofluorescence with anti- $\beta$ -galactosidase antibody. As shown in Fig. 5, the fusion protein expressed from plasmid pt1- $\beta$ Gal, which contains residues GRKKR of Tat, was observed predominantly in the nucleus. In contrast, the fusion protein expressed from plasmid pt2- $\beta$ Gal, which contains the second stretch of positively charged amino acids including the sequence QRRP, was for the most part localized in the cytoplasm. Similar results were obtained with a staining procedure that measured functional  $\beta$ -galactosidase activity (not shown).

**Monomeric form of Tat can form metal-protein complexes.** The presence of a cysteine-rich region within the *tat* protein is reminiscent of putative zinc- or metal-binding fingers present in some transcriptional regulatory proteins (10, 14,

21). The cysteines present in Tat have the potential to form different structural configurations with metal in either the monomeric or dimeric form. Recently, Frankel et al. have shown that Tat can form a stable dimer configuration in the presence of divalent cations (9).

To examine the ability of the monomeric form of Tat and the cysteine substitution mutants to bind metal, the DNA fragments encoding these mutations were excised from the eucaryotic expression vector and cloned into the procaryotic expression vector pictured in Fig. 2. A similar level of Tat expression was observed with each Tat derivative following IPTG induction in *E. coli* (Fig. 6A). The ability of each protein to bind metal was addressed by electrophoretic transfer of protein to nitrocellulose membranes, followed by incubation with  $^{65}\text{ZnCl}_2$ . This procedure has been used to identify other zinc-binding proteins (23). As illustrated in Fig. 6B, both the authentic and mutant *tat* proteins retained their ability to bind zinc under these conditions. Thus, it is unlikely that loss of biological activity reflects the ability of the monomeric form of Tat to bind zinc.

## DISCUSSION

In the present study, site-directed mutagenesis was used to identify functional domains within the HIV *tat* protein. The *tat* protein was localized predominantly in the nucleus, in accord with previously published results (11). Moreover, accumulation within the nucleolus was observed. The nucleolar localization is likely to be real, since parallel experiments performed with a *c-fos* protein and nuclear  $\beta$ -galactosidase expression vector gave clear nuclear staining and nucleolar exclusion. The nucleolar localization of Tat may provide clues towards understanding its mechanism of action, which at present remains unclear. Since at least one component of the mechanism of Tat function is thought to involve posttranscriptional events, localization within the nucleolus would be consistent with mechanisms that involve mRNP formation or RNA processing or transport. Similar mechanisms have been proposed for another HIV transacting protein, Rev (regulator of virion protein expression, previously referred to as *artItrS*), which also accumulates in the nucleolus (unpublished data). Alternatively, if transactivation occurs via an indirect mechanism, one may speculate that intermediates of this pathway are present in the nucleolus.

By alteration of individual amino acids, three potential functional domains within the *tat* protein were identified. The first region critical for Tat function is present at the amino-terminal end. Deletion of the first three amino acids led to normal subcellular localization, although the ability to transactivate was lost. It is noteworthy that this substitution removed one of the three negatively charged (glutamic acid) residues present in the protein.

The second set of mutations were made within the highly conserved cysteine-rich region. Mutations were made in which cysteines 22, 27, and 37 were changed to serine and cysteine 25 was changed to arginine. With each of these proteins, normal expression and proper subcellular localization were retained, but transactivation was abolished. It has been proposed that the cysteine-rich domain has the potential to form a zinc finger common to several other transcriptional regulatory proteins (10, 14, 21). Frankel et al. have proposed an alternative structure that is distinct from a zinc-binding finger and is involved in metal-linked dimer formation (9). Regardless of the configuration of the cysteines in the native molecule, our results clearly emphasize

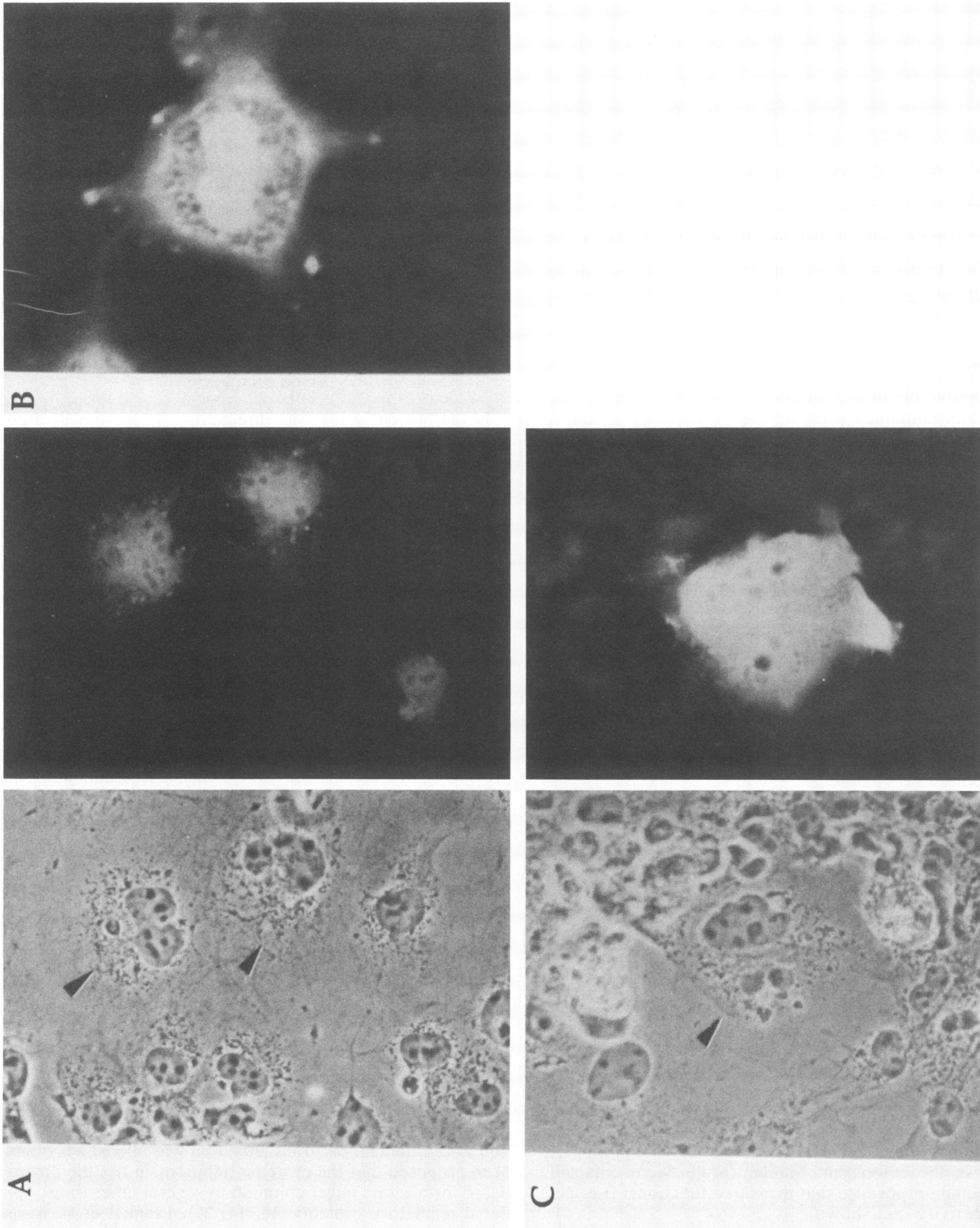


FIG. 5. Localization of  $\beta$ -galactosidase fusion proteins. COS cells were transfected with plasmids p1- $\beta$ Gal (A and B) and p12- $\beta$ Gal (C). At 48 h posttransfection, cells were fixed and permeabilized, and the subcellular localization of the fusion proteins was determined by indirect immunofluorescence with anti- $\beta$ -galactosidase antibody. No phase-contrast micrograph is shown for the cells in panel B.

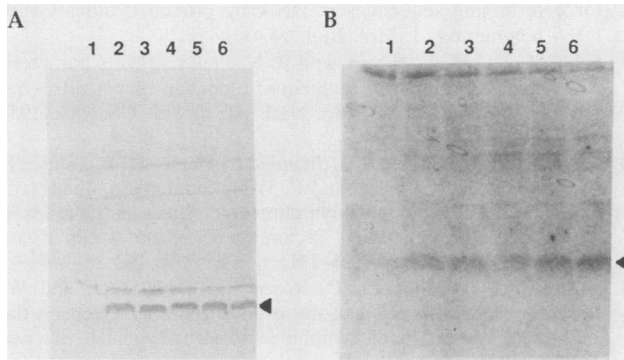


FIG. 6. Zinc-65 binds to Tat. *E. coli* cells expressing Tat were lysed, and proteins were separated by SDS-PAGE. Proteins were electrophoretically transferred to nitrocellulose. The nitrocellulose filter was first treated with  $^{65}\text{ZnCl}_2$  and then visualized by autoradiography (B). The filter was then washed extensively to remove zinc and blotted with anti-*tat* antibody plus conjugated goat anti-rabbit alkaline phosphatase (A). Lanes: Control *E. coli* lysate (lane 1), control lysate obtained from *E. coli* expressing authentic *tat* protein (lane 2), pC22 (lane 3), pC25 (lane 4), pC27 (lane 5), pC37 (lane 6). Arrows indicate *tat* protein.

the importance of the individual cysteine residues for biological function. In addition, the ability of Tat and the cysteine substitution derivatives to form metal-protein complexes indicates that loss of function cannot be attributed to the ability of the monomeric form of Tat to bind metal under these conditions. Further analysis of the cysteine region, in particular the ability of the mutant cysteine substitution derivatives to form metal-linked dimers, is in progress.

The last group of *tat* mutations centered on the stretch of positively charged amino acids present between residues 48 and 56. Although Tat function was retained with these alterations, the activity of the individual mutants was markedly diminished. Mutant pKK5051 had only minor activity compared with the wild-type *tat* protein. Although protein was expressed, as evidenced by transactivation, indirect immunofluorescence failed to detect substantial levels of Tat in the nucleus. No activity was detected with plasmid pK50-S, which has a stop codon at amino acid 50. Thus, residues between positions 50 and 58 are required for function (24).

To examine further the role of the basic residues, their ability to function as a nuclear localization signal was examined. We found that a  $\beta$ -galactosidase fusion protein that contained the sequence GRKKR from the *tat* protein at the amino-terminal end of  $\beta$ -galactosidase accumulated within the nucleoplasm. In contrast, mutant proteins carrying amino-terminal fusions with the QRRP sequence corresponding to the second cluster of basic residues within Tat were, for the most part, localized in the cytoplasm. Therefore, it seems likely that the GRKKR sequence, or a part of this sequence, functions as a nuclear localization signal. This result is not surprising, considering that stretches of basic residues have been reported to serve a similar function in other nuclear proteins (12).

Since each of the proteins with mutations in the basic stretch demonstrated some degree of transactivation, it is likely that a proportion of *tat* protein accumulates within the nucleus. As each of the Tat derivatives contained only one or two amino acid alterations, it is possible that residues present in the second cluster of charged amino acids may substitute for those deleted within the true localization signal, although in themselves they do not serve the same

function. It is noteworthy that the  $\beta$ -galactosidase fusion proteins accumulated within the nucleus and were excluded from the nucleolus, whereas the *tat* protein accumulated within the nucleolus. This raises the possibility that Tat contains a distinct nucleolar localization signal or that the intrinsic structure of the protein controls localization.

In summary, our results suggest that the small 14-kDa *tat* protein is a complex protein with at least three distinct functional domains. Further studies on the precise role of the individual functional regions should aid in our understanding of the mechanism of transactivation.

#### ACKNOWLEDGMENTS

We thank Nahum Sonnenberg and Sophie Roy for the gift of *tat* antibody, Reiner Gentz for plasmid pDS56RBS11-1, Richard Chiz-zonite, Paulo Ferreira, and James Hempstead for advice on immunofluorescence, Tom Curran for the *c-fos* vector, Robert Crowl for the *E. coli lacZ* gene, and Bryan Cullen for helpful discussion.

W.A.H. was supported by Public Health Service grant CA42098 from the National Institutes of Health.

#### LITERATURE CITED

1. Arya, S. K., C. Guo, S. F. Josephs, and F. Wong-Staal. 1985. *trans*-Activator gene of human T-lymphotropic virus type III (HTLV-III). *Science* **229**:69-73.
2. Bujard, H., R. Gentz, M. Lanzer, D. Stueber, M. Mueller, I. Ibrahimi, M. T. Haeupte, and B. Dobberstein. 1987. A T5 promoter based transcription-translation system for the analysis of protein *in vitro* and *in vivo*. *Methods Enzymol.* **155**:416-433.
3. Burglin, T. R., and E. M. DeRoberts. 1987. The nuclear migration signal of *Xenopus laevis* nucleoplasm. *EMBO J.* **6**:2617-2625.
4. Cullen, B. R. 1986. *trans*-Activation of human immunodeficiency virus occurs via a bimodal mechanism. *Cell* **46**:973-982.
5. Cullen, B. R. 1987. Use of eukaryotic expression technology in the functional analysis of cloned genes. *Methods Enzymol.* **152**:684-704.
6. Dayton, A. I., J. G. Sodroski, C. A. Rosen, W. C. Goh, and W. A. Haseltine. 1986. The *trans*-activator gene of the human T cell lymphotropic virus type III is required for replication. *Cell* **44**:941-947.
7. Feinberg, M. B., R. F. Jarrett, A. Aldovini, R. C. Gallo, and F. Wong-Staal. 1986. HTLV-III expression and production involve complex regulation at the levels of splicing and translation of viral RNA. *Cell* **46**:807-817.
8. Fisher, A. G., A. Aldovini, C. Debouk, R. C. Gallo, and F. Wong-Staal. 1986. The transactivator gene of HTLV-III is essential for virus replication. *Nature (London)* **320**:367-371.
9. Frankel, A. D., D. S. Bredt, and C. O. Pabo. 1988. *tat* protein from immunodeficiency virus forms a metal-linked dimer. *Science* **240**:70-73.
10. Harthorne, T. A., H. Blumberg, and E. T. Young. 1986. Sequence homology of the yeast regulatory protein ADR1 with *Xenopus* transcription factor TFIIIA. *Nature (London)* **320**:283-287.
11. Hauber, J., A. Perkins, E. P. Heimer, and B. R. Cullen. 1987. *trans*-Activation of human immunodeficiency virus gene expression is mediated by nuclear events. *Proc. Natl. Acad. Sci. USA* **84**:6364-6368.
12. Kalderson, D., B. L. Roberts, W. D. Richardson, and A. E. Smith. 1984. A short amino acid sequence able to specify nuclear location. *Cell* **39**:499-509.
13. Kao, S. Y., A. F. Calman, P. A. Luciw, and B. M. Peterlin. 1987. Anti-termination of transcription within the long terminal repeat of HIV-1 by *tat* gene product. *Nature (London)* **330**:489-493.
14. Miller, J., A. D. McLachlan, and A. Klug. 1985. Repetitive zinc-binding domains in the protein transcription factor IIIA from *Xenopus* oocytes. *EMBO J.* **4**:1609-1614.
15. Muesing, M. A., D. H. Smith, and D. J. Capon. 1987. Regulation of mRNA accumulation by a human immunodeficiency virus *trans*-activator protein. *Cell* **48**:691-701.

16. Mulligan, R. C., B. H. Howard, and P. Berg. 1979. Synthesis of rabbit  $\beta$ -globin in cultured monkey kidney cells following infection with an SV40- $\beta$ -globin recombinant genome. *Nature (London)* **277**:108-114.
17. Nisbet, I. T., and M. W. Beilharz. 1985. Simplified DNA manipulations based on *in vitro* mutagenesis. *Gene Anal. Technol.* **2**:23-29.
18. Peterlin, B. M., P. A. Luciw, P. J. Barr, and M. D. Walker. 1986. Elevated levels of mRNA can account for the *trans*-activation of human immunodeficiency virus. *Proc. Natl. Acad. Sci. USA* **83**:9734-9738.
19. Rosen, C. A., J. G. Sodroski, W. C. Goh, A. I. Dayton, J. Lippke, and W. A. Haseltine. 1986. Post-transcriptional regulation accounts for the *trans*-activation of human T-lymphotropic virus type III. *Nature (London)* **319**:555-559.
20. Rosen, C. A., J. G. Sodroski, and W. A. Haseltine. 1985. The location of *cis*-acting regulatory sequences in the human T cell lymphotropic virus type III (HTLV-III/LAV) long terminal repeat. *Cell* **41**:813-823.
21. Rosenberg, U. B., C. Schroder, A. Preiss, A. Kienlin, S. Cote, I. Riede, and H. Jackle. 1986. Structural homology of the product of the *Drosophila kruppel* gene with *Xenopus* transcription factor IIIA. *Nature (London)* **319**:336-339.
22. Sanger, F., S. Nicklen, and A. R. Coulson. 1975. A rapid method for determining sequences in DNA by primed synthesis with DNA polymerase. *J. Mol. Biol.* **94**:441-451.
23. Schiff, L. A., M. L. Nibert, and B. N. Fields. 1988. Characterization of a zinc blotting technique: evidence that a retroviral *gag* protein binds zinc. *Proc. Natl. Acad. Sci. USA* **85**:4195-4199.
24. Seigel, L. J., L. Ratner, S. J. Josephs, D. Derse, M. B. Feinberg, G. R. Reyes, S. J. Obriez, and F. Wong-Staal. 1986. Transactivation induced by human T-lymphotropic virus type III maps to a viral sequence encoding 58 amino acids and lacks tissue specificity. *Virology* **148**:226-231.
25. Sodroski, J., R. Patarca, C. Rosen, F. Wong-Staal, and W. Haseltine. 1985. Location of the *trans*-activating region on the genome of human T-cell lymphotropic virus type III. *Science* **229**:74-77.
26. Wood, W. I., J. Gitshier, L. A. Lasky, and R. M. Lawn. 1985. Base composition-independent hybridization in tetramethylammonium chloride: a method for oligonucleotide screening of highly complex gene libraries. *Proc. Natl. Acad. Sci. USA* **82**:1585-1588.
27. Wright, C. M., B. K. Felber, N. Paskalis, and G. N. Pavlakis. 1986. Expression and characterization of the *trans*-activator of HTLV-III/LAV virus. *Science* **234**:988-992.